

ANALYSIS OF THE DUALITY OF THREE PHASE PWM CONVERTERS WITH DC VOLTAGE LINK AND DC CURRENT LINK

JOHANN W. KOLAR, HANS ERTL and FRANZ C. ZACH

Technical University Vienna, Power Electronics Section
Gußhausstraße 27, Vienna, AUSTRIA

Abstract

Duality relationships are of special importance in physics and especially in electrical engineering and allow the extension or unification of the theory. This makes possible the transfer of mathematical relationships and dimensioning guidelines and of other system oriented principles derived for one system to the dual system.

In this paper the duality of three-phase PWM converters with DC current and DC voltage link is analyzed by the means of space vector calculus for the example of a forced commutated rectifier system. The power-invariant transformation of the converter phase voltages or line currents into complex image quantities (space vectors) allows the presentation of the converter system as a complex space-vector voltage-source or current-source; its initial value has to be defined by the switching status of the converter system. The modulation principles (e.g., optimized pulse patterns) known from converters with DC voltage link, guidelines concerning the dimensioning of power circuit components and considerations relating to control can thereby simply be transferred to DC current link converters.

Introduction [1], [2]

Due to essential progress in the power semiconductor area (realization of (voltage controlled) turn-off devices) and in the area of signal processing electronics (microprocessors and signal processors) PWM converter systems have experienced broad application in industry. Thereby the DC voltage link PWM converters has gained major importance. It can be applied as well in drive applications as in mains applications (PWM rectifier, static Var-compensator).

The structure of the power circuit of a DC voltage link PWM converter is shown in Fig.1. Coupling of the three-phase (poly-phase) AC system and the DC system is achieved (depending on the system switching status) by semiconductor devices (electrical valves) which are bidirectional regarding current flow but unidirectional regarding blocking voltage. Due to the time-discontinuous system operation energy storage devices have to be applied on the AC side and on the DC side in order to make the exchange of harmonic power (at pulse frequency) possible. Dependent on the specific application (see before) thereby the inductances on the AC side have to be visualized as being realized by the stray inductances of the AC machine used. The three-phase voltage system is then formed (according to a simple equivalent circuit) by the counter-emf system of the machine. The inductances have to be explicitly connected in series if the application is given as mains converter. Basically the AC side current shape can be freely set by a corresponding voltage balance for the magnetic storage elements (inductances). For sinusoidal currents

the (instantaneous) power flow into the DC link remains constant; thereby the power flow is related to the fundamental and is possible in both directions. This, in connection with the remarks made before, would make possible the avoidance of the energy storage elements described; this would require infinitely high converter switching frequency and would be equivalent to the realization of an ideal power electronic converter.

Due to the basic problems of bidirectional conversion between three-phase and DC energy by power electronic systems (especially due to the convincing properties of the converter system described) one has to pose the basic question of possible derivation of other applicable structures. As one possibility, as treated here, one can use the duality approach because it allows the transfer of the system behavior to the dual system (here especially the behavior concerning the energy conversion or the power flow related to the terminal behavior is of interest).

Here, in general a conclusion valid for circuit C is transferred into a dual conclusion, valid for circuit C_d . Thereby duality relationships are applied which are defined in detail in the following. Considering electrical circuits duality relationships exist concerning the structure (topology of the graph) and concerning the elements (devices) of the circuit.

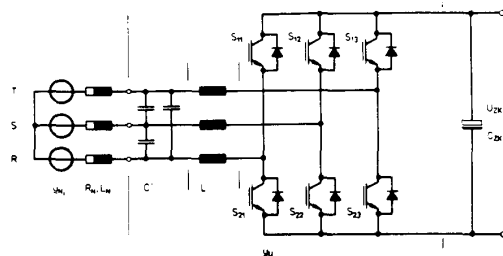


Fig.1: Structure of the power circuit of a three-phase DC voltage link converter system

Fundamentals of Duality Relations [3], [4], [5], [6]

A condition for the existence of a graph being dual with respect to a given graph is its planar property (i.e., being representable in a plane without crossings). This condition is necessary and sufficient if the original graph does not contain any of the KURATOWSKY-Graphs (shown in Fig.2) as sub-graphs. If the term *graph* is extended to *network* (or, in general, to *net*), one has to add further (quantitative) properties to the purely structural (graph-theoretical) relationships. This means that network ele-

ments or, in connection with the definition of a positive direction (directed graph), the quantities (voltages, currents) describing the physical properties have to be related to points and curves.

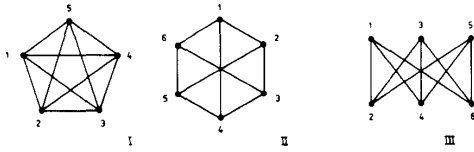


Fig. 2: Graphs according to KURATOWSKY (I,II). The "supply graph" III follows by redrawing of II.

For deriving the network being dual to a given network to each area of the plane enclosed by branches a node of the dual network is related. Furthermore, one more node is placed in the plain outside of the (original) network graph. The nodes of the dual network are connected with each other such that each branch of the original network is intersected by exactly one branch of the dual network. The transfer of the directional sense is performed by rotating the directed branch of the original network in the given positive rotational direction until the branch mentioned coincides with the corresponding branch of the dual network. To each branch of the dual network finally a network element is related which is dual to the corresponding network element of the given network.

The reversible duality relations can be briefly summarized as follows:

- *Topological relations:*
 - node — loop
 - parallel connection — series connection
 - delta connection — star connection
- *Power sources:*
 - voltage source — current source
- *Physical quantities:*
 - voltage — current
 - voltage time area — current time area
 - (magnetic flux — electrical charge)
- *Network (Circuit) elements:*
 - capacitor — inductor
 - resistor — resistor (conductance)

For a clear explanation of the approach the development of a network being dual to a simplified, schematized power electronic circuit is described (see Fig.3). Thereby the magnetic and electrical storage elements are replaced by current and voltage sources. In this connection the question not discussed so far regarding the replaceability of an electrical valve arises.

Basically one only can give a first step by replacing the properties characterizing the switching status of a valve by dual properties (e.g., transfer from forward current to reverse blocking voltage). Thereby, e.g., a conducting valve is transferred into a blocking valve in the dual network. By this approach as well the entire network topology as the switching states (motoring — freewheeling — braking, i.e. feeding back into the energy source) is directly transferred into corresponding ones of the dual network (see Fig.3a).

A further possibility is given by considering the partial structures existing for the different switching states and by their dual replacement (see Fig.3b). The function of the devices thereby is implicitly connected to the topology of these partial graphs. The connection of the different partial structures has to be done (in order to be unique) via arrangement of switching elements in a minimum effort approach; thereby it shall be possible to derive all dual partial networks from the structure of the entire dual network via corresponding switching states. It has to be

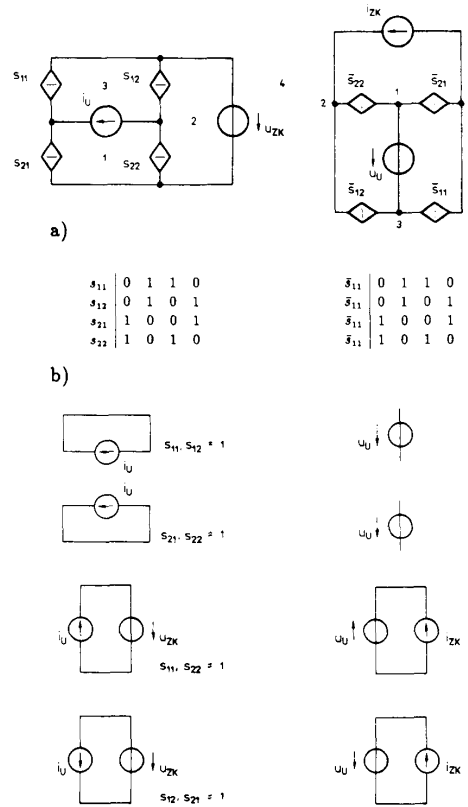


Fig. 3: Development of a network being dual to a simplified single-phase DC voltage link converter

pointed out that the direction of power flow remains unchanged when turning from a primal network to a dual network. This proves the invariance of power and energy flow relative to the duality principle.

We now consider that in the previously discussed and very much simplified structure of a one phase bridge circuit the switching elements are realized by inserting transistors and diodes (Fig.4). Then the valves which in the primal network are bidirectional concerning current flow and unipolar concerning blocking voltage turn into unidirectional valves concerning current flow and bipolar valves concerning blocking voltage. (Thereby the unipolar elements concerning blocking voltage in the primal network are realized by transistor and diode in antiparallel, the bipolar valves concerning blocking voltage in the dual network

are realized by a series connection of transistor and diode.) Furthermore, for these considerations in general on the DC side a restriction of the system operating region to two quadrants in the u - i -plane is made.

transformation of the entire network is hindered by the nonplanarity of the original network. It contains, as seen by comparing with Fig.2, a KURATOWSKY-Graph (the "supply graph") as sub-graph. For different switch positions, however, the network

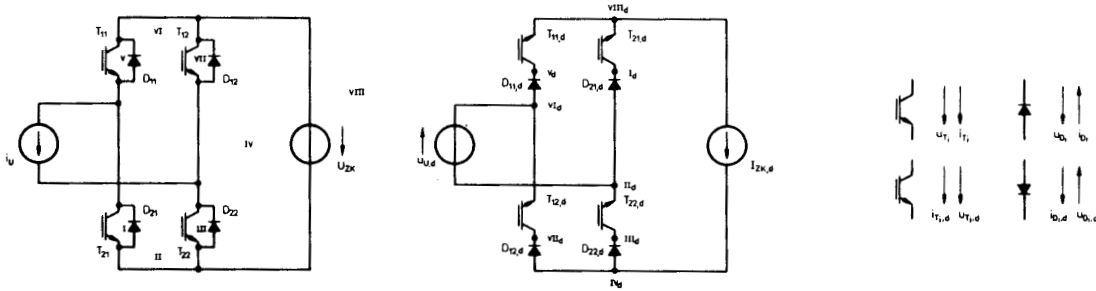


Fig.4: Structure of the power electronic circuits of Fig.3 being dual with respect to each other. Thereby the switching elements are realized by combination of transistors and diodes.

After these short discussions of the basics of duality relations now we want to turn to the main problem of deriving a structure being dual to the DC voltage link PWM converter. For the sake of simplicity we again will consider the configuration where the energy storage elements are replaced by current and voltage sources (see Fig.5a). Thereby the immediate dual

falls into planar partial structures whose dual relations can be given immediately (Fig.5b). A minimum effort combination of the dual partial systems can be found by the overall structure shown in Fig.5c. The function of a bridge leg of the primal network can be represented by a two-way switch between positive and negative voltage bus; therefore the structure consisting of

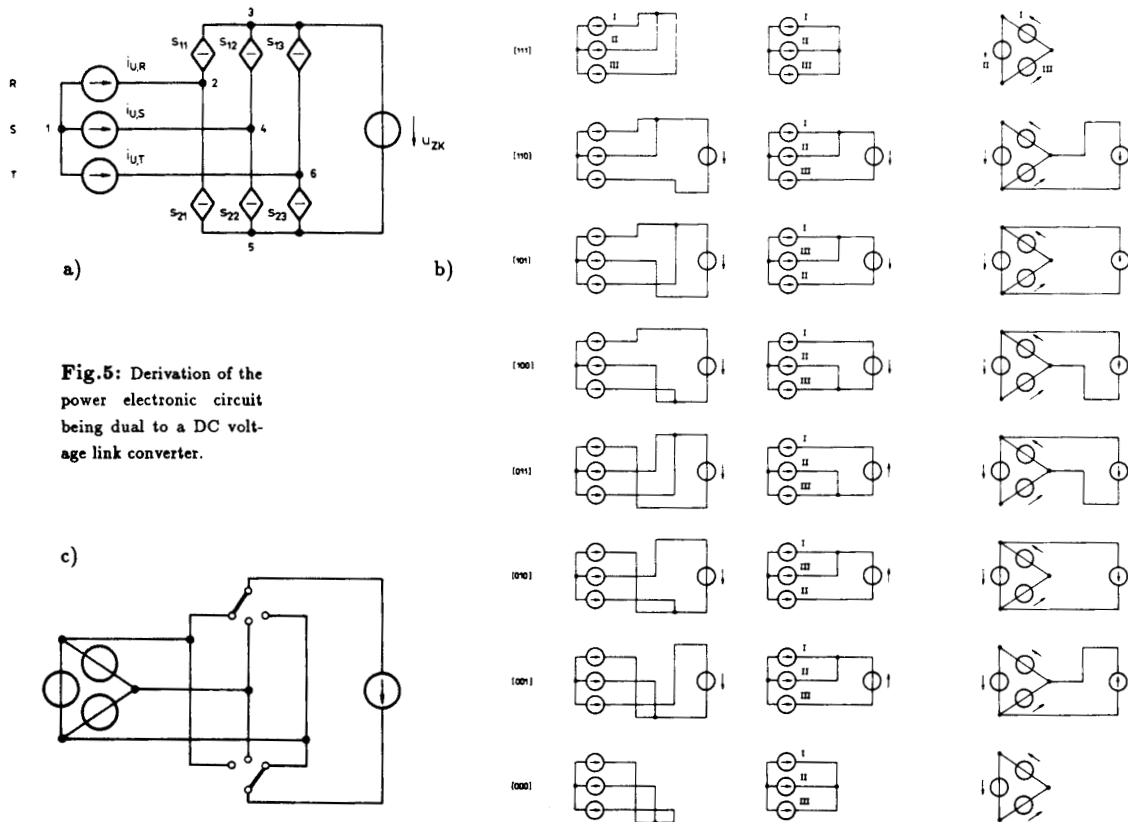


Fig.5: Derivation of the power electronic circuit being dual to a DC voltage link converter.

three two-way switches turns into a structure consisting of two three-way switches. For realization by combinations of transistors and diodes the statements made before for one phase bridge circuits are again applicable.

A comparison of the primal and the dual network shows immediately that the dual transformation turns the PWM converter system with DC voltage link into one with DC current link. This is also the case because (as mentioned) the relations concerning power conversion between AC and DC side are invariant with respect to the duality relation. DC current link and DC voltage link PWM converter systems therefore show a very close relationship which is given by the duality relations.

The simple transfer of the given theory of the DC voltage link converter system made thereby possible in the following is briefly discussed using a comparison of the mathematical description of both systems. Of special interest thereby is the possibility to transfer all modulation methods developed for the DC voltage link PWM converter (e.g., off-line optimized pulse patterns). This is made possible by the immediate relation of the switching states of the systems. Furthermore, one can immediately apply the quantities determining the system stress after proper normalization to dimensioning the dual system. (These quantities in most cases will have been gained by digital simulation.) For the sake of brevity and clarity of this paper this aspect shall be left to a discussion in a future paper, however.

Mathematical Description of the DC Voltage Link PWM Converter System [7], [8]

Due to the discontinuous system operation each valve can be connected with a binary switching function $s_{ij} = 0, 1$. Thereby the indices define the semiconductor position within the converter structure (Fig.1). The different switching functions are combined into a switching matrix

$$\mathbf{S}(t) = \begin{bmatrix} s_{11}(t) & s_{12}(t) & s_{13}(t) \\ -s_{21}(t) & -s_{22}(t) & -s_{23}(t) \end{bmatrix} \quad (1)$$

(whereby according to Fig.6 always one and only one of the switching functions of any particular bridge leg has the value 1, see Fig.14). Then with

$$\mathbf{u}_U(t) = \begin{bmatrix} u_{U,R}(t) \\ u_{U,S}(t) \\ u_{U,T}(t) \end{bmatrix}, \quad (2)$$

$$\mathbf{i}_U(t) = \begin{bmatrix} i_{U,R}(t) \\ i_{U,S}(t) \\ i_{U,T}(t) \end{bmatrix}, \quad (3)$$

$$\mathbf{e} = \begin{bmatrix} 1 \\ 1 \end{bmatrix}, \quad (4)$$

we have

$$\mathbf{u}_U(t) = \frac{1}{2} U_{ZK} \mathbf{S}^T(t) \mathbf{e}, \quad (5)$$

$$\mathbf{i}_{ZK}(t) = \mathbf{S}(t) \mathbf{i}_U(t), \quad (6)$$

$$\mathbf{i}_{ZK}(t) = i_{ZK}(t) \mathbf{e}, \quad (7)$$

$$i_{ZK} = \frac{1}{2} \mathbf{e}^T \mathbf{i}_{ZK}. \quad (8)$$

These equations describe the "image" of the AC side currents in the DC link current and also the formation of the converter output voltage based on the DC link voltage for any instant of

time. Therefore the power conversion by the converter system is completely described by the switching (status) matrix \mathbf{S} .

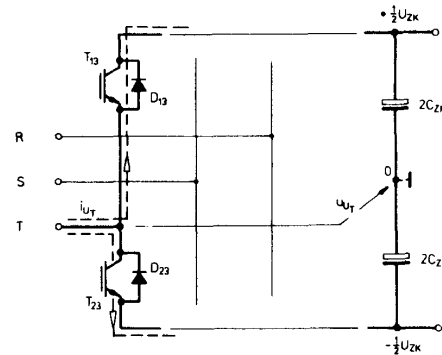


Fig.6: Possibility of functional replacement of a bridge leg of a DC voltage link converter by a two-way switch between positive and negative DC link rail.

We now assume that the description of the system behavior for switching frequencies high with respect to the output frequency is related to mean values over the pulse period. Then the switching functions s_{ij} are transformed according to

$$\alpha_{ij}(\tau) = \frac{1}{T_P} \int_{T_P} s_{ij}(t_\mu) dt_\mu, \quad \alpha_{ij} \leq 1 \quad (9)$$

into equivalent duty ratios $\alpha_{ij}(\tau)$. These duty ratios are related to the time position τ of the pulse interval within the fundamental period. This is equivalent to turning from the analysis of the partial system structures valid for the different switching states to the quasi-continuous behavior of the overall structure. This in turn is equivalent to assuming infinitely high switching frequency. Equation (1) now becomes

$$\mathbf{A}(\tau) = \begin{bmatrix} \alpha_{11}(\tau) & \alpha_{12}(\tau) & \alpha_{13}(\tau) \\ -\alpha_{21}(\tau) & -\alpha_{22}(\tau) & -\alpha_{23}(\tau) \end{bmatrix}. \quad (10)$$

Thereby the two-way switching function of the bridge leg has to be included by the conditions

$$\begin{aligned} \alpha_{11}(\tau) + \alpha_{21}(\tau) &= 1, \\ \alpha_{12}(\tau) + \alpha_{22}(\tau) &= 1, \\ \alpha_{13}(\tau) + \alpha_{23}(\tau) &= 1. \end{aligned} \quad (11)$$

Analogous to Eqn.(5-8) now the description of the converter function is given by

$$\mathbf{u}_U(\tau) = \frac{1}{2} U_{ZK} \mathbf{A}^T(\tau) \mathbf{e} \quad (12)$$

and

$$\mathbf{i}_{ZK}(\tau) = \mathbf{A}(\tau) \mathbf{i}_U(\tau). \quad (13)$$

The assumption of appropriate duty ratios thereby immediately determines as well the output current as the input voltage amplitude. This follows also from a simple power balance considering the lack of energy storage elements.

We now assume sinusoidal shapes of the AC side currents and voltages (stationary operation)

$$\begin{aligned}
u_{U,R}(\tau) &= \hat{U}_U \cos \varphi_U, \\
u_{U,S}(\tau) &= \hat{U}_U \cos \left(\varphi_U - \frac{2\pi}{3} \right), \\
u_{U,T}(\tau) &= \hat{U}_U \cos \left(\varphi_U + \frac{2\pi}{3} \right), \\
\varphi_U &= \omega_U \tau, \\
i_{U,R}(\tau) &= \hat{I}_U \cos (\varphi_U + \varphi), \\
i_{U,S}(\tau) &= \hat{I}_U \cos \left(\varphi_U - \frac{2\pi}{3} + \varphi \right), \\
i_{U,T}(\tau) &= \hat{I}_U \cos \left(\varphi_U + \frac{2\pi}{3} + \varphi \right), \\
\varphi &= \varphi_{\underline{u}_U, i_U}.
\end{aligned} \tag{14}$$

$$\begin{aligned}
i_{U,R}(\tau) &= \hat{I}_U \cos (\varphi_U + \varphi), \\
i_{U,S}(\tau) &= \hat{I}_U \cos \left(\varphi_U - \frac{2\pi}{3} + \varphi \right), \\
i_{U,T}(\tau) &= \hat{I}_U \cos \left(\varphi_U + \frac{2\pi}{3} + \varphi \right), \\
\varphi &= \varphi_{\underline{u}_U, i_U}.
\end{aligned} \tag{15}$$

$$\varphi = \varphi_{\underline{u}_U, i_U}. \tag{16}$$

Then we have with

$$M = \frac{2\hat{U}_U}{U_{ZK}} \quad m(\tau) = \frac{2u_U(\tau)}{U_{ZK}} \tag{17}$$

for the modulation functions of the different phases

$$\begin{aligned}
m_R &= M \cos \varphi_U, \\
m_S &= M \cos \left(\varphi_U - \frac{2\pi}{3} \right), \\
m_T &= M \cos \left(\varphi_U + \frac{2\pi}{3} \right).
\end{aligned} \tag{18}$$

These are projected via the modulation method into duty ratios

$$\begin{aligned}
\alpha_{11}(\tau) &= \frac{1}{2} [1 + m_R(\tau)], \\
\alpha_{12}(\tau) &= \frac{1}{2} [1 + m_S(\tau)], \\
\alpha_{13}(\tau) &= \frac{1}{2} [1 + m_T(\tau)].
\end{aligned} \tag{19}$$

According to

$$i_{ZK}(\tau) = \alpha_{11} i_{U,R} + \alpha_{12} i_{U,S} + \alpha_{13} i_{U,T}, \tag{20}$$

$$i_{ZK}(\tau) = \frac{1}{2} m_R i_{U,R} + \frac{1}{2} m_S i_{U,S} + \frac{1}{2} m_T i_{U,T}, \tag{21}$$

the resulting DC link current follows as

$$i_{ZK}(\tau) = \frac{3}{4} \hat{I}_U M \cos \varphi. \tag{22}$$

It shows therefore a time-invariant value, related to the time-invariant power flow of a symmetrical three-phase system.

Besides the phase related description (via switching matrix \mathbf{S}) now a presentation of the system behavior can be performed with minimum effort and power-invariant via transformation of the phase quantities into a space vector \underline{s} lying in a complex plane according to

$$\underline{s} = \frac{1}{U_{ZK}} \underline{u}_U \quad |\underline{s}| = \frac{2}{3}, \tag{23}$$

$$\begin{aligned}
\underline{u}_U &= \frac{2}{3} [u_{U,R} + a u_{U,S} + a^2 u_{U,T}], \\
|\underline{u}_U| &= \frac{2}{3} U_{ZK},
\end{aligned} \tag{24}$$

$$\begin{aligned}
a &= \exp \left(j \frac{2\pi}{3} \right), \\
a^2 &= \exp \left(-j \frac{2\pi}{3} \right).
\end{aligned}$$

The decoupling of the zero sequence system (homopolar system) given thereby presents no limitation for the treatment of three-wire systems.

According to the basic operation of the different bridge legs as two-way switches (reversing switches) between positive and negative DC link voltage bus the number of possible converter switching states can be simply given by

$$\bar{V}_{n,i} = n^i = 2^3 = 8 \tag{25}$$

(see also Figs.7 and 8). Equation (25) gives the variation of $n = 2$ elements for the $i = 3^{\text{rd}}$ class (phase number) with repetitions.

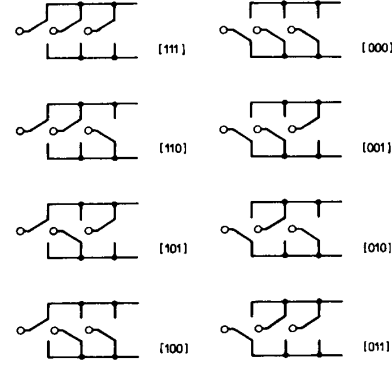


Fig.7: Possible switch positions of a DC voltage link converter system.

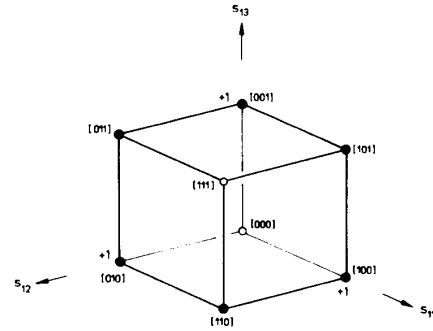


Fig.8: Insertion of possible switching states in the space of phase switching functions ("switching state cube").

A denomination of the switching status is simply possible via only the first line of the switching matrix or by its interpretation as binary number via its decimal equivalent, respectively. The space vectors related to the different switching states are given via

$$\underline{s} = \begin{cases} 0 \\ \frac{2}{3} \exp \left(j k \frac{\pi}{3} \right) \quad k = 1 \dots 6 \end{cases} \tag{26}$$

or by Fig.10a, respectively. Thereby the two freewheeling states (000) and (111) of the system show vanishing magnitude of the space vector (equivalent to a "decoupling" of the AC and DC systems).

With the definition of the converter input current space vector

$$\dot{i}_U = \frac{2}{3} (\dot{i}_{U,R} + \dot{a} \dot{i}_{U,S} + \dot{a}^2 \dot{i}_{U,T}) \quad (27)$$

the system function (cf. Eqs.(5-8)) is described via

$$\dot{u}_U = \dot{z} U_{ZK}, \quad (28)$$

$$\dot{i}_{ZK} = \frac{3}{2} \Re \{ \dot{z} \dot{i}_U \}. \quad (29)$$

For the DC link currents appearing for the different switching states we have

$$\begin{aligned} [000] : & \quad \dot{i}_{ZK} = 0 \\ [001] : & \quad \dot{i}_{ZK} = \dot{i}_T \\ [010] : & \quad \dot{i}_{ZK} = \dot{i}_S \\ [011] : & \quad \dot{i}_{ZK} = -\dot{i}_R \\ [100] : & \quad \dot{i}_{ZK} = \dot{i}_R \\ [101] : & \quad \dot{i}_{ZK} = -\dot{i}_S \\ [110] : & \quad \dot{i}_{ZK} = -\dot{i}_T \\ [111] : & \quad \dot{i}_{ZK} = 0 \end{aligned} \quad (30)$$

Besides being applicable to a general description of the converter function the space vector calculus (originally developed

for analysis of the transient behavior of AC machines) also proves applicable to the formulation of the equations characterizing the dynamical behavior of power electronic systems. We now want to apply this principle to the PWM rectifier system where the filter capacitances C' are included in order to make possible later an immediate comparison to a dual DC current link PWM rectifier system (see Fig.9). For the dynamic system equations there follows when replacing the delta-connected capacitances C' by the equivalent star-connection with $C = 3C'$

$$\begin{aligned} \dot{i}_N - \dot{i}_U &= C \frac{d\dot{u}_N}{dt}, \\ \dot{u}_N - \dot{u}_U &= L \frac{d\dot{i}_U}{dt}, \\ C_{ZK} \frac{d\dot{u}_{ZK}}{dt} &= \dot{i}_{ZK} - \dot{i}_L - \frac{\dot{u}_{ZK}}{R_L}. \end{aligned} \quad (31)$$

These equations can be represented as simple equivalent circuit according to Fig.10.

When representing the stationary operation and specializing to purely sinusoidal system movements the system behavior description by space vectors turns into AC circuit analysis with phasor representation of the quantities. The vectors show con-

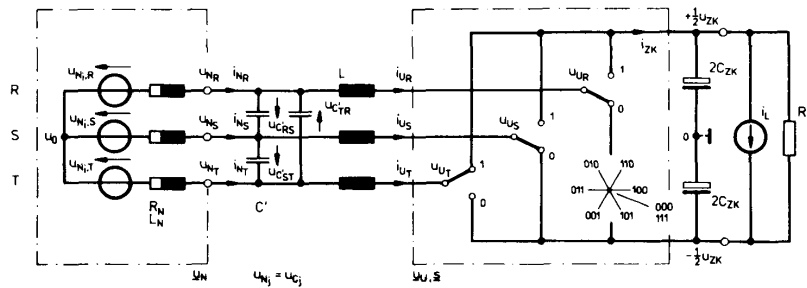


Fig.9: Structure of the power circuit of a PWM rectifier system for functional replacement of the bridge legs.

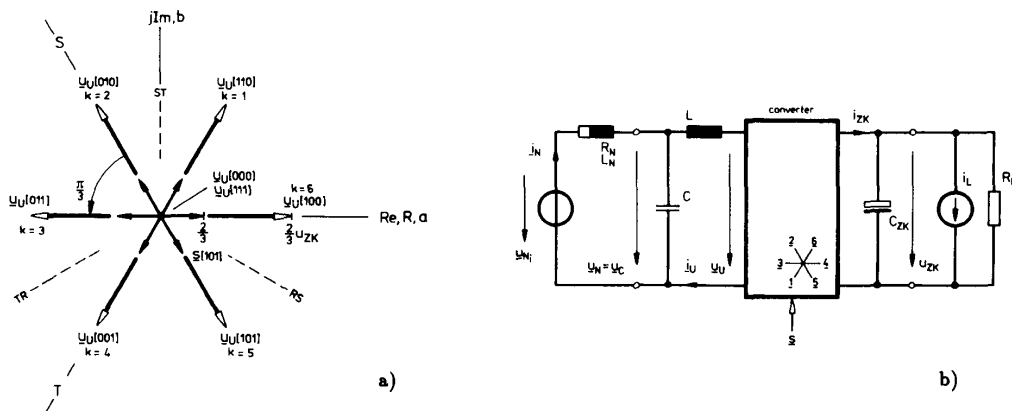


Fig.10: a) Converter voltage space vector and b) space vector equivalent circuit for the DC voltage link converter system.

stant magnitude and constant angular speed. With

$$\underline{u}_N = \hat{U}_N \exp(j\varphi_N) \quad \varphi_N = \omega_N t, \quad (32)$$

$$\underline{Z} = R + j\omega L = Z \exp\left[j\left(\frac{\pi}{2} - \rho\right)\right] \quad (33)$$

we have for the mains current vector

$$\underline{i}_{N,dq} = \frac{1}{Z} (\underline{u}_{N,dq} - \underline{u}_{U,dq}) \exp\left[-j\left(\frac{\pi}{2} - \rho\right)\right] \quad (34)$$

as described in a d, q -coordinate system related to the mains voltage (and rotating). For the sake of simplicity the capacitances C have been omitted. The relationship can be illustrated as circle diagram of the system (see Fig.11, specialized for $R=0$). The relative position of the mains current vector (and with it immediately the real and reactive mains power relations) can be given via a change of the amplitude (modulation M) and position (angle δ) of the converter output voltage.

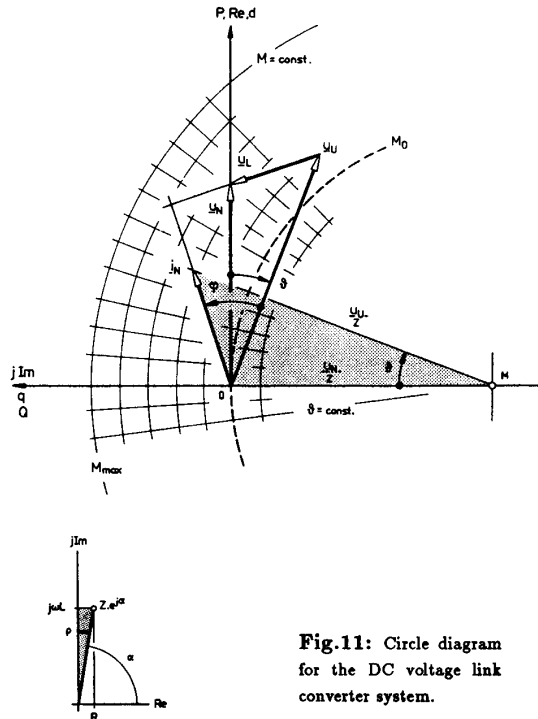


Fig.11: Circle diagram for the DC voltage link converter system.

Mathematical Description of the DC Current Link PWM Converter System [9], [10], [11], [12], [13]

Completely analogous to the DC voltage link PWM converter system the function of the DC current link PWM converter (see Fig.12) can be given (again) by a switching matrix according to

$$\underline{i}_U(t) = I_{ZK} \mathbf{S}^T(t) \mathbf{e}, \quad (35)$$

$$\underline{u}_{ZK}(t) = \begin{bmatrix} u_{ZK,II}(t) \\ u_{ZK,II}(t) \end{bmatrix}, \quad (36)$$

$$\underline{u}_{ZK}(t) = \mathbf{S}(t) \underline{u}_U(t), \quad (37)$$

$$\frac{1}{2} \underline{u}_{ZK}(t) = \frac{1}{2} e^T \underline{u}_{ZK}. \quad (38)$$

The current commutation for the DC current link converter operates not within one bridge leg between upper and lower DC link bus ("on the DC side") but it operates between the different phases (i.e., "on the AC side" — see Fig.13). However, using this statement for a classification of converters into systems with AC and DC side commutation might lead to problems concerning the proper use of duality terms ([16], [6]). Complete system controllability is only given if always only one switching function of the upper and lower bridge half shows the value 1 (see Fig.14). This is because for turning on more than one valve in one bridge half the combination of valves with the highest line-to-line voltages would conduct the current. This condition is turned into

$$\begin{aligned} \alpha_{11}(\tau) + \alpha_{12}(\tau) + \alpha_{13}(\tau) &= 1, \\ \alpha_{21}(\tau) + \alpha_{22}(\tau) + \alpha_{23}(\tau) &= 1 \end{aligned} \quad (39)$$

when considering the mean values for a pulse period. For the system description we then have (cf. Eqs.(8, 12, 13))

$$\underline{i}_U(\tau) = I_{ZK} \mathbf{A}^T(\tau) \mathbf{e}, \quad (40)$$

$$\underline{u}_{ZK}(\tau) = \mathbf{A}(\tau) \underline{u}_U(\tau), \quad (41)$$

$$\frac{1}{2} \underline{u}_{ZK}(\tau) = \frac{1}{2} e^T \underline{u}_U(\tau). \quad (42)$$

Based on (purely) sinusoidal shape of the AC side currents and voltages

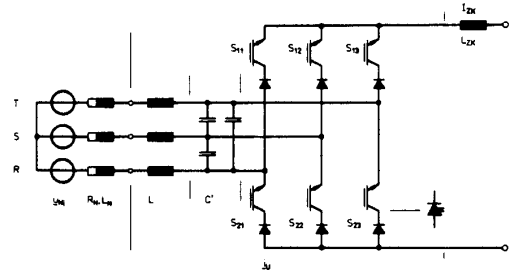


Fig.12: Power circuit structure for the DC current link converter system

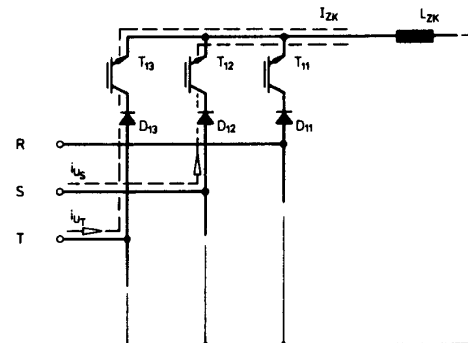


Fig.13: Possibility of functional replacement of a bridge half of a DC current link converter via a three-way switch between the phase branches.

$$\begin{aligned}
i_{U,R}(\tau) &= \hat{I}_U \cos \varphi_I, \\
i_{U,S}(\tau) &= \hat{I}_U \cos \left(\varphi_I - \frac{2\pi}{3} \right), \\
i_{U,T}(\tau) &= \hat{I}_U \cos \left(\varphi_I + \frac{2\pi}{3} \right), \\
\varphi_I &= \omega_U \tau,
\end{aligned} \tag{43}$$

$$\begin{aligned}
u_{U,R}(\tau) &= \hat{U}_U \cos(\varphi_I + \varphi), \\
u_{U,S}(\tau) &= \hat{U}_U \cos \left(\varphi_I - \frac{2\pi}{3} + \varphi \right), \\
u_{U,T}(\tau) &= \hat{U}_U \cos \left(\varphi_I + \frac{2\pi}{3} + \varphi \right), \\
\varphi &= \varphi_{\underline{u}, \underline{i}_U},
\end{aligned} \tag{44}$$

we have with

$$M = \frac{\hat{I}_U}{I_{ZK}} \quad m(\tau) = \frac{i_U(\tau)}{I_{ZK}} \tag{45}$$

for the modulation functions of the different phases

$$\begin{aligned}
m_R &= M \cos \varphi_U, \\
m_S &= M \cos \left(\varphi_U - \frac{2\pi}{3} \right), \\
m_T &= M \cos \left(\varphi_U + \frac{2\pi}{3} \right).
\end{aligned} \tag{46}$$

These are projected via the modulation method into corresponding duty cycles. The resulting DC link voltage follows according to

$$u_{ZK}(\tau) = (\alpha_{11} - \alpha_{21}) u_{U,R} + (\alpha_{12} - \alpha_{22}) u_{U,S} + (\alpha_{13} - \alpha_{23}) u_{U,T}, \tag{47}$$

$$u_{ZK}(\tau) = m_R u_{U,R} + m_S u_{U,S} + m_T u_{U,T} \tag{48}$$

to

$$u_{ZK}(\tau) = \frac{3}{2} M \hat{U}_U \cos \varphi. \tag{49}$$

It shows a constant value which is related to the time-invariant power flow. Comparison with Eq.(22) immediately shows the close relationship of both systems. The different multiplier of the equations is caused by the definition of the modulation depth of the DC current link converter (see Eq.(45)).

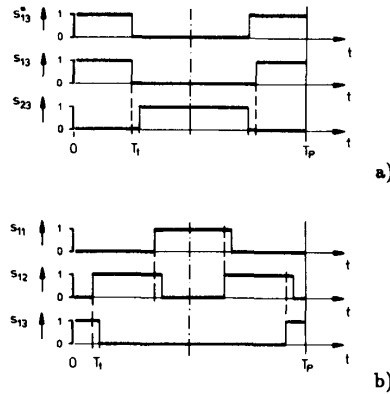


Fig.14: Derivation of the control signals for the valves of a) DC voltage link converter or b) DC current link converter, respectively, based on a given modulation function.

Besides the phase related description now the description of the system behavior can be performed again by using a switching status space vector

$$\underline{s} = \frac{1}{I_{ZK}} \underline{i}_U, \tag{50}$$

$$\begin{aligned}
\underline{i}_U &= \frac{2}{3} (i_{U,R} + \underline{a} i_{U,S} + \underline{a}^2 i_{U,T}), \\
|\underline{i}_U| &= \frac{2}{\sqrt{3}} I_{ZK}.
\end{aligned} \tag{51}$$

The possible system switching states can be calculated according to the three-way switch operation between the different phases via

$$\bar{V}_{n,i} = n^i = 3^2 = 9. \tag{52}$$

(This represents the variation of $n = 3$ elements (phase number) for the $i = 2^{\text{nd}}$ class with repetitions.) The denomination of the switching status has to be performed here by the entire switching matrix. The space vectors related to the different switching states are given by

$$\underline{s} = \begin{cases} 0 \\ \frac{2}{\sqrt{3}} \exp \left(\frac{\pi}{6} + k \frac{\pi}{3} \right) \end{cases} \quad k = 1 \dots 6 \tag{53}$$

or by Fig.15a, respectively. There exist three freewheeling states of the system ($u_{ZK} = 0$). With the definition of the converter input current space vector (Eq.(51)) the system function can be described via

$$\underline{i}_U = \underline{s} I_{ZK}, \tag{54}$$

$$u_{ZK} = \frac{3}{2} \Re \{ \underline{s}^* \underline{u}_U \} \tag{55}$$

(cf. Eqs.(28, 29)). For the DC link voltages valid for the different switchings states we have

$$\begin{aligned}
\begin{bmatrix} 100 \\ 100 \end{bmatrix} &: u_{ZK} = 0 \\
\begin{bmatrix} 010 \\ 010 \end{bmatrix} &: u_{ZK} = 0 \\
\begin{bmatrix} 001 \\ 001 \end{bmatrix} &: u_{ZK} = 0 \\
\begin{bmatrix} 001 \\ 010 \end{bmatrix} &: u_{ZK} = u_T - u_S \\
\begin{bmatrix} 010 \\ 100 \end{bmatrix} &: u_{ZK} = u_S - u_R \\
\begin{bmatrix} 001 \\ 100 \end{bmatrix} &: u_{ZK} = u_T - u_R \\
\begin{bmatrix} 100 \\ 001 \end{bmatrix} &: u_{ZK} = u_R - u_T \\
\begin{bmatrix} 100 \\ 010 \end{bmatrix} &: u_{ZK} = u_R - u_S \\
\begin{bmatrix} 010 \\ 001 \end{bmatrix} &: u_{ZK} = u_S - u_T
\end{aligned} \tag{56}$$

Based on Fig.16 there follows for the description of the dynamic behavior

$$\begin{aligned}
\underline{i}_N - \underline{i}_U &= C \frac{d\underline{u}_U}{dt}, \\
\underline{u}_N - \underline{u}_U &= L \frac{d\underline{i}_N}{dt},
\end{aligned} \tag{57}$$

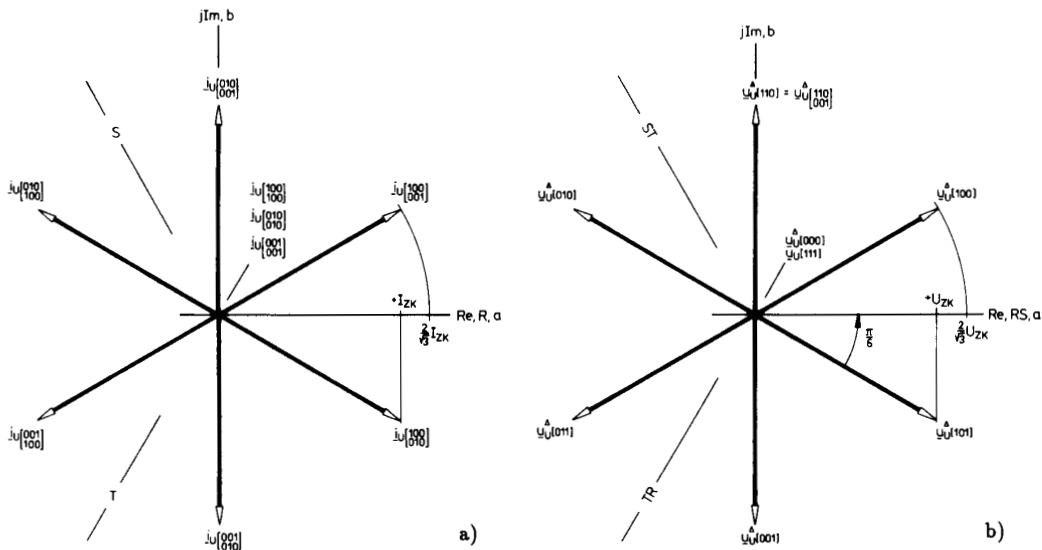


Fig.15: Correspondence of the dual switching states of a) DC voltage link converter or b) DC current link converter, respectively, via comparison of the space vectors given for different switching matrices for converter line-to-line output voltage and for converter output current space vector.

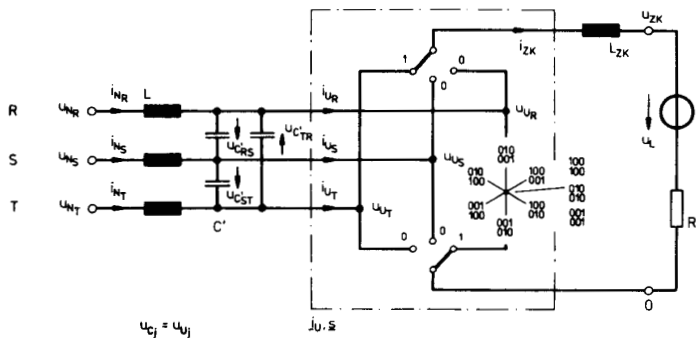


Fig.16: Power circuit structure of a DC current link converter for functional replacement of the bridge halves.

$$L_{ZK} \frac{di_{ZK}}{dt} = u_{ZK} - u_L - i_{ZK} R_L \quad (58)$$

(cf. Fig.9 or Eqs.(31), respectively). The representation of the equations given as space vector equivalent circuit leads to Fig.17 (cf. Fig.10).

Figure 18 shows the description of the stationary operation related to the fundamental via a circle diagram (cf. Fig.11). Absolute value and position of the mains current vector defining the mains power relations can be given by the converter current vector. For the sake of simplicity the mains voltage is thought to be impressed directly across the capacitances C' (see Fig.16); phase difference $\pi/2$ between mains voltage phasor and capacitor current phasor).

Duality Relations of the Switching States of DC Current and DC Voltage Link PWM Converter [14], [15], [16], [17], [18]

Because there exists a multitude of (optimized) modulation methods for the DC voltage link converter, the determination of the duality relations of the switching states between primal and dual systems is of special interest. With the knowledge of the duality relations the modulation method can then be transferred directly without further calculations.

The relation of the switching states (corresponding switching state matrices) is determined via comparison of the possible converter voltage space vectors (or current space vectors, respectively) of both systems (see Fig.15). Thereby according to the duality of star and delta connections the description of the system function of the DC voltage link converter has to be per-

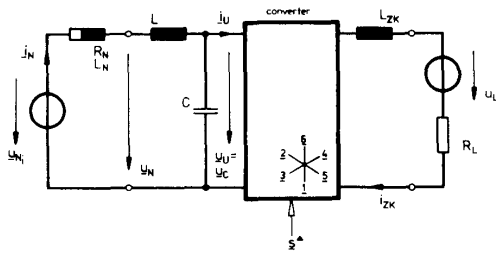


Fig.17: Space vector equivalent circuit for the DC current link converter.

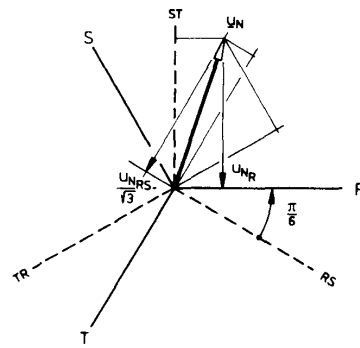


Fig.19: Reverse transformation of the space vector into line-to-line and phase quantities.

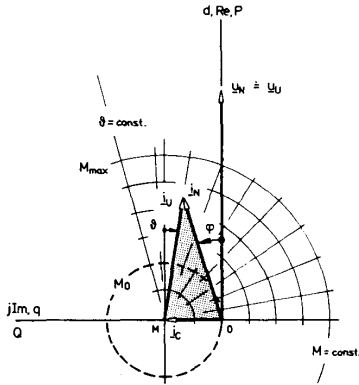


Fig.18: Circle diagram of the DC current link converter.

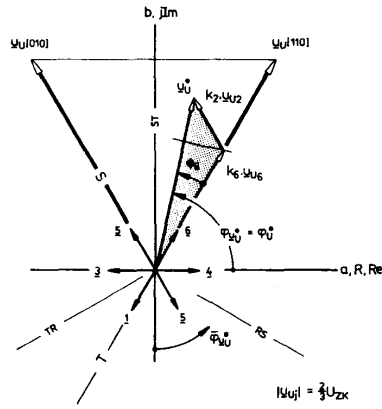


Fig.20: Representation of the converter output voltage reference space vector via switching between neighbouring converter output voltage vectors.

formed using the space vector of the line-to-line voltages (see Fig.19)

$$\underline{u}_U^\Delta = \frac{2}{3} (u_{U,RS} + a u_{U,ST} + a^2 u_{U,TR}) ,$$

$$\underline{u}_U^\Delta = (1 - a^2) \underline{u}_U , \quad (59)$$

$$|u_U^\Delta| = \frac{2}{\sqrt{3}} U_{ZK} . \quad (60)$$

In connection with Eq.(53) (switching status space vector of DC current link converter) then the \$\underline{u}_U^\Delta\$ can be formulated according to

$$\underline{u}_U^\Delta = \underline{s} U_{ZK} . \quad (61)$$

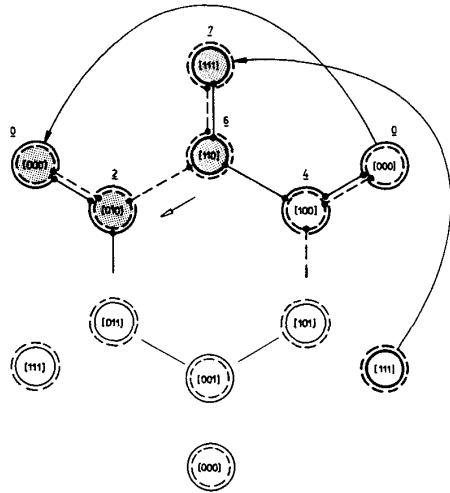
The basic function of the converter system in general consists in the stationary case in the approximation of a reference-value space vector of constant magnitude and rotating with constant angular speed by discrete converter (current, voltage) space vectors over a pulse period (see Fig.20). The then given cyclic sequence of switching states (shown in Fig.21a) of the DC voltage link converter system then corresponds directly to the sequence of dual switching states of the related DC current link converter system (Fig.21b). One has to observe, however, that starting with a switching status forming the output current with a minimum number of switchings there can be reached two freewheeling states (and not only one as for the DC voltage link converter). This gives a further degree of freedom for the mod-

ulation method. Basically one has to incorporate again possible freewheeling states considering equal stress of the different valves into the overall cycle of the switching status sequence, however (as, e.g., shown in Fig.21b in dual relation to Fig.21a).

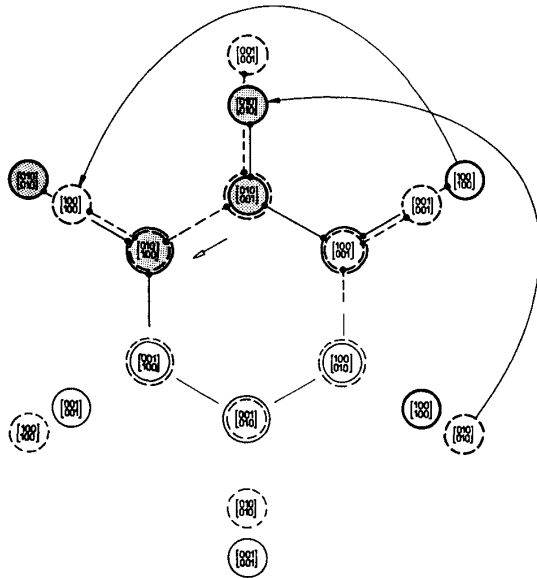
The derivation of the dual switching states is illustrated once more in Fig.22 based on a pulse width modulation method given for a DC voltage link converter. These dual switching states can simply be read either from Fig.21 or from the shape of the line-to-line converter output voltage (normalized to the DC link voltage). Figure 23 shows (corresponding to Fig.22) the trajectory of the related converter voltage integral or of the dual converter current integral, respectively (dual correspondence of voltage-time area and of current-time area).

If there arises the problem to derive a modulation method for given phase reference values of the DC current link converter applying the duality relations it can be solved simply according to

$$m_{U_{ZK,R}} = \frac{2}{3} (m_{I_{ZK,R}} - m_{I_{ZK,T}}) ,$$



a)



b)

Fig.21: Switching sequence of a) DC voltage link converter or b) DC current link converter, respectively.

$$\begin{aligned}
 m_{UZK,S} &= \frac{2}{3}(m_{1ZK,S} - m_{1ZK,R}) , \\
 m_{UZK,T} &= \frac{2}{3}(m_{1ZK,T} - m_{1ZK,S}) .
 \end{aligned}
 \tag{62}$$

Thereby Eqs.(17, 19 and 45) have to be considered and proper recoding has to be performed (see Figs.21,24). However, for a modulation (control) method based on space vector quantities one can use directly the knowledge of the current space vectors occurring for the different switching states (function of the system as space vector current source). Thereby the "detour" via phase quantities (modulation functions) can be avoided.

Conclusions

As this paper shows, DC voltage link converter and DC current link converter systems show a close relationship defined by the duality relation of electrical networks. Basically these make possible (due to the possibility of transferring the equations characterizing the behavior of one system to the dual system) to unify the theory of power electronic systems. Furthermore, a deepened understanding of the system function is made possible. The presentation given in the literature in detailed form so far only for DC-DC converters can be extended to power electronic energy converters in general. Thereby one has to especially observe the application of terms consistent with duality definitions.

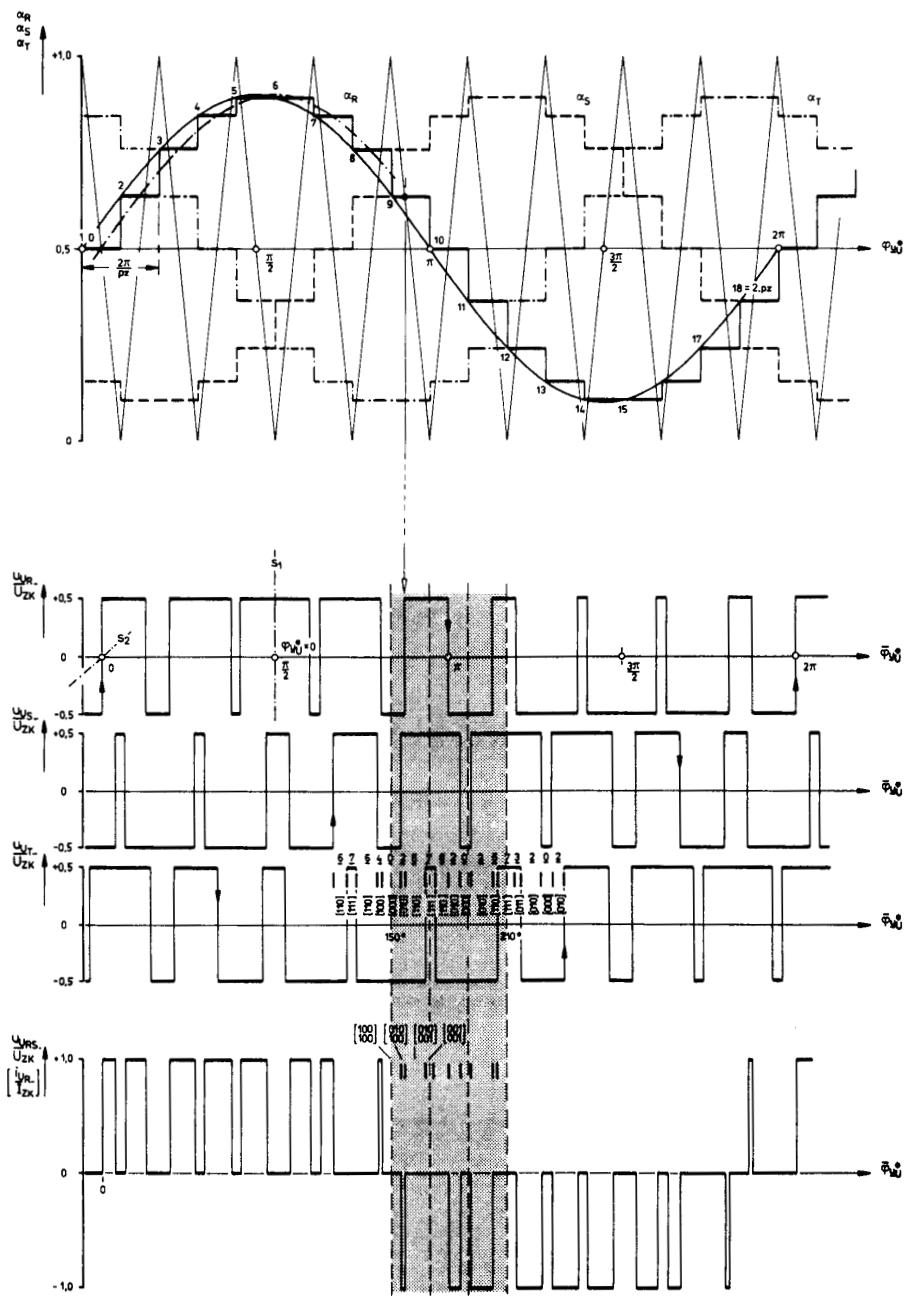


Fig.22: Modulation method (asymmetric regular sampling) for a DC voltage link converter and its transfer to a DC current link converter (analysis of the line-to-line voltages).

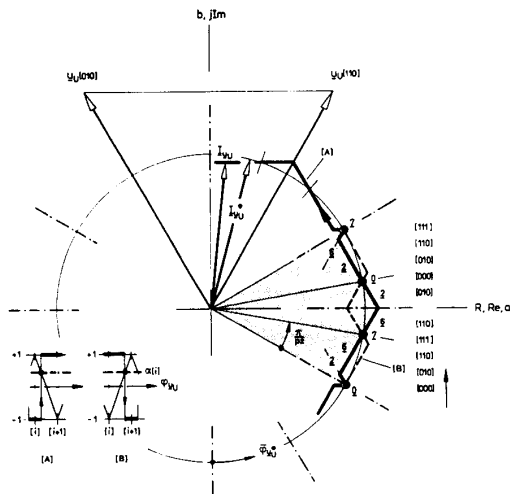


Fig. 23: Trajectory of the converter voltage space vector integral or current space vector integral, respectively, corresponding to Fig. 22.

	}	$\begin{bmatrix} 100 \\ 100 \end{bmatrix}$
$\begin{bmatrix} 000 \\ 100 \end{bmatrix}$		$\begin{bmatrix} 010 \\ 010 \end{bmatrix}$
$\begin{bmatrix} 001 \end{bmatrix}$	—	$\begin{bmatrix} 001 \\ 001 \\ 010 \end{bmatrix}$
$\begin{bmatrix} 010 \end{bmatrix}$	—	$\begin{bmatrix} 010 \\ 100 \end{bmatrix}$
$\begin{bmatrix} 011 \end{bmatrix}$	—	$\begin{bmatrix} 001 \\ 100 \end{bmatrix}$
$\begin{bmatrix} 100 \end{bmatrix}$	—	$\begin{bmatrix} 100 \\ 001 \end{bmatrix}$
$\begin{bmatrix} 101 \end{bmatrix}$	—	$\begin{bmatrix} 100 \\ 010 \end{bmatrix}$
$\begin{bmatrix} 110 \end{bmatrix}$	—	$\begin{bmatrix} 010 \\ 001 \end{bmatrix}$

Fig. 24: Duality relations of the switching states.

References

[1] **A. Busse, J. Holtz, Multiloop Control of a Unity Power Factor Fast Switching AC to DC Converter**, Proceedings of the 13th PESC, Cambridge, MA, June 14–17, 1982, pp. 171–179.

[2] **H. Ertl, J. W. Kolar, F. C. Zach, Analysis of Different Current Control Concepts for Forced Commutated Rectifier (FCR)**, Proceedings of the 11th PCI, Munich, West Germany, June 17–19, 1986, pp. 195–217.

[3] **E. Rummich, Graphen und ihre Anwendung in der Elektrotechnik**, Automatisierungstechnische Schriftenreihe, Österr. Produktivitäts-Zentrum, Oktober 1969, Wien.

[4] **S. Čuk, General Topological Properties of Switching Structures**, Proceedings of the 10th PESC, San Diego, CA, June 18–22, 1979, pp. 109–130.

[5] **K.-H. Liu, F. C. Lee, Topological Constraints on Basic PWM Converters**, Proceedings of the 19th PESC, Kyoto, Japan, April 11–14, 1988, pp. 164–172.

[6] **E. Blumenschein, Dualitätsgerechte Begriffe für die Leistungselektronik**, Elektrische, Berlin, Jg. 42, 1988, H. 7, pp. 267–270.

[7] **T. Salzmann, A. Weschta, Progress in Voltage Source Inverters and Current Source Inverters**, Conference Record of IAS Annual Meeting, Atlanta, GA, October 18–23, 1987, Part 1, pp. 577–583.

[8] **A. Weschta, Pulse-Controlled Current-Source Inverters with Turn-Off Semiconductor Devices**, Proceedings of the 2nd European Conference on Power Electronics, Grenoble, France, September 22–24, 1987, Vol. 1, pp. 377–382.

[9] **L. Malesani, P. Tenti, Three-Phase AC/DC PWM Converter with Sinusoidal AC Currents and Minimum Filter Requirements**, IEEE Transactions on IA, Vol. IA-23, No. 1, January/February 1987, pp. 71–77.

[10] **K. Kaltenbach, Modulationsverfahren mit Raumzeigern für Stromzwischenkreis-Pulswechselrichter**, ETZ-Archiv, Bd. 10, 1988, H. 9, pp. 303–306.

[11] **M. Hombu, S. Ueda, A. Ueda, A Current Source GTO Inverter with Sinusoidal Inputs and Outputs**, Conference Record of IAS Annual Meeting, Toronto, Canada, October 6–11, 1985, pp. 1033–1039.

[12] **S. R. Doradla, S. K. Mandal, A Three-Phase AC-to-DC Power Transistor Converter-Controlled DC Motor Drive**, IEEE Transactions on IA, Vol. IA-23, No. 5, September/October 1987, pp. 848–854.

[13] **S. Fukuda, N. Takada, PWM Current Source Rectifier with Sinusoidal Line Current**, Conference Record of IAS Annual Meeting, Atlanta, GA, October 18–23, 1987, Part 1, pp. 679–684.

[14] **F. C. Zach, A New Pulse Width Modulation Control for Line Commutated Converters Minimizing the Mains Harmonics Content**, 6th Symposium on Electromagnetic Compatibility, Zürich, Switzerland, March 5–7, 1985, pp. 545–550.

[15] **L. Abraham, F. Koppelman, Die Zwangskommütierung, ein neuer Zweig der Stromrichtertechnik**, ETZ-A, Jg. 87, 1966, pp. 649–658.

[16] **K. Heumann, Elektrotechnische Grundlagen der Zwangskommütierung**, E. und M., Jg. 84, 1967, H. 3, pp. 99–112.

- [17] **H. P. Beck, M. Michel**, *Die gleichspannungsseitige Kommutierung bei netzgeführten Stromrichtern*, Archiv für Elektrotechnik 65, 1982, pp. 245-250.
- [18] **M. F. Schlecht**, *Harmonic-Free Utility/DC Power Conditioning Interfaces*, IEEE Transactions on PE, Vol. PE-1, No. 4, October 1986, pp. 231-239.

ACKNOWLEDGEMENT

The authors are very much indebted to the Austrian FONDS ZUR FÖRDERUNG DER WISSENSCHAFTLICHEN FORSCHUNG who supports the work of the Power Electronics Section at their university.